We are IntechOpen, the world's leading publisher of Open Access books Built by scientists, for scientists

4,800
Open access books available

122,000
International authors and editors

135M
Downloads

Our authors are among the

154
Countries delivered to

TOP 1%
most cited scientists

12.2%
Contributors from top 500 universities

WEB OF SCIENCE™

Selection of our books indexed in the Book Citation Index in Web of Science™ Core Collection (BKCI)

Interested in publishing with us?
Contact book.department@intechopen.com

Numbers displayed above are based on latest data collected.
For more information visit www.intechopen.com

12

Wave Propagation in Carbon Nanotubes

Lifeng Wang, Haiyan Hu and Wanlin Guo
Nanjing University of Aeronautics and Astronautics
China

1. Introduction

Interest in carbon nanotubes has grown rapidly since their discovery (Iijima, 1991). A single-walled carbon nanotube can be considered as a single layer graphite sheet rolled into cylinder. Three examples of single-walled carbon nanotubes, armchair, zigzag and chiral, are shown in Figure 1 (Qian *et al.*, 2002). A multi-walled carbon nanotube is similar to a single-walled carbon nanotube, but with many layers of graphite sheets in the cylinder structure.

Recent studies have indicated that carbon nanotubes exhibit superior mechanical and electronic properties over any known materials, and hold substantial promise for new super-strong composite materials, among others. For instance, carbon nanotubes have an exceptionally high elastic modulus (Treacy *et al.*, 1996), and sustain large elastic strain and failure strain (Yakobson *et al.*, 1996; Wong *et al.*, 1997). Apart from an extensive experimental study to characterize the mechanical behavior of carbon nanotubes, theoretical or computational modeling of carbon nanotubes has received considerable attention. The current computational modeling approaches include both atomistic modeling and continuum modeling.

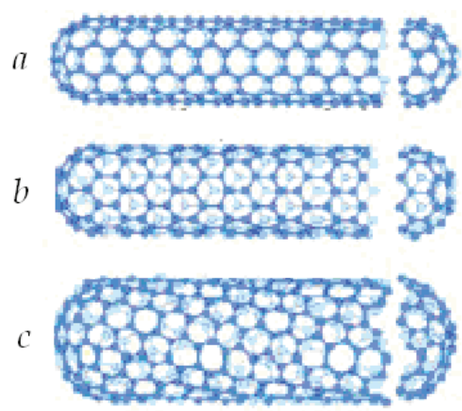

Fig. 1. Examples of carbon nanotubes, (a) armchair, (b) zigzag and (c) chiral ((Qian *et al.*, 2002))

Among the researches of continuum modeling of carbon nanotubes, numerous studies concentrated on the static mechanical behavior, such as buckling, of carbon nanotubes by using the elastic models of beam and cylindrical shell (Qian *et al.*, 2002). Several research

Source: Wave Propagation in Materials for Modern Applications, Book edited by: Andrey Petrin,
ISBN 978-953-7619-65-7, pp. 526, January 2010, INTECH, Croatia, downloaded from SCIYO.COM

teams implemented the elastic models of beam to study the dynamic problems, such as vibration and wave propagation (Poncharal *et al*., 1999; Popov *et al*., 2000; Yoon *et al*., 2002, 2003a,b), of carbon nanotubes. Some other teams used the elastic models of cylindrical shell to study the vibration and wave dispersion relations of carbon nanotubes (Wang *et al*., 2005a; Dong & Wang, 2006; Natsuki *et al*. 2005, 2006). Furthermore, Chakraborty (2007) modeled a multi-walled carbon nanotube as an assemblage of cylindrical shell elements connected throughout their lengths by distributed springs to investigate the elastic waves of very high frequency in carbon nanotubes, and to give the dispersion relation between the group velocity and the wave number. Their studies showed that both elastic models of beam and cylindrical shell are valid to describe the vibration or wave propagation of carbon nanotubes in a relatively low frequency range.

In recent years, the need to describe the microstructure-dominated behavior of a mechanical component in an averaged sense, without modeling detailed microstructures and deformation processes at the micro-scale, has stimulated numerous studies on enriched continuum models. In these models, the nonstandard deformation and force quantities account for the influences of the microstructures on mechanical behaviors. The description of the deformation behavior of solids is not limited to relations between elastic stresses and strains. The consideration of microstructure, which is usually neglected in the classical theory of elasticity, results in the constitutive law related to the strain gradient (Mindlin, 1964). This constitutive law, different from the generalized Hook's law, enables one to predict many new phenomena, such as the dispersive waves in non-local elastic continuum, owing to the microstructures in a solid. As a consequence, the wave propagation and dispersion in granular media have also drawn considerable attention (Manolis, 2000; Chang & Gao, 1995). For instance, the wave propagation in a rod exhibiting non-local elasticity has become an interesting topic (Nowinski, 1984; Mühlhaus & Oka, 1996; Askes et al, 2002). Several researchers (Sudak, 2003; Zhang et al., 2004, 2005; Wang, 2005b; Wang *et al*., 2006a; Xie *et al.* 2006) established the non-local elastic models with the second order gradient of stress taken into account so as to describe the vibration and wave propagation of both single- and multi-walled carbon nanotubes in a higher frequency range. The molecular dynamics simulations showed those models worked much better than the elastic models in a relatively high frequency range. However, the molecular dynamics simulations also showed that the micro-structures of a carbon nanotube might have a so significant influence on the waves of very high frequency such that non-elastic models could not predict the wave dispersion well (Wang & Hu, 2005; Wang et al. 2006b).

The primary objective of this work is to study the phase velocity and group velocity of the flexural and longitudinal wave propagations in carbon nanotubes so as to examine the effect of micro-structures of a carbon nanotube on the wave dispersion. This work deals with the dispersion relations of both longitudinal and flexural waves in single-walled and multi-walled carbon nanotubes via the non-local elastic models of both Timoshenko beams and cylindrical shells. The study focuses on the comparison between the non-local elastic models and the elastic models in predicting the dispersion relation. For this purpose, Section 2 presents the molecular dynamics modeling of carbon nanotubes. Section 3 presents the dispersion relation of longitudinal waves in a single-walled carbon nanotube from a non-local elastic model of cylindrical shell, which includes the second order gradient of strain in order to characterize the micro-structures of the carbon nanotube. Section 4 gives the dispersion relation of flexural waves in a single-walled carbon nanotube by using a non-

local elastic model of Timoshenko beam. Section 5 turns to the dispersion relation of flexural waves in a multi-walled carbon nanotube from a non-local elastic model of multi-Timoshenko beams, which also takes the second order gradient of strain into account. Similarly, Section 6 gives the dispersion relation of longitudinal waves in a multi-walled carbon nanotube on the basis of a non-local elastic model of multi-cylindrical shells. Finally, the chapter ends with some concluding remarks made in Section 7.

2. Molecular dynamics model for carbon nanotubes

This section presents the molecular dynamics models for wave propagation in a carbon nanotube, respectively, for a wide range of wave numbers. Molecular dynamics simulation consists of the numerical solution of the classical equations of motion, which for a simple atomic system may be written

$$m_i \ddot{\mathbf{r}}_i = \mathbf{F}_i = -\frac{\partial V}{\partial \mathbf{r}_i}. \tag{1}$$

For this purpose the force $\mathbf{F}_i$ acting on the atoms are derived from a potential energy, $V(r_{ij})$ where r_{ij} is the distance from atom *i* to atom *j*.

In the molecular dynamics models of this chapter, the interatomic interactions are described by the Tersoff-Brenner potential (Brenner, 1990), which has been proved applicable to the description of mechanical properties of carbon nanotubes. The structure of the Tersoff-Brenner potential is as follows

$$V(r_{ij}) \equiv \sum_i \sum_{j(>i)} [V_R(r_{ij}) - \overline{B}_{ij} V_A(r_{ij})], \tag{2}$$

$V_R(r_{ij})$ and $V_A(r_{ij})$ are the repulsive and attractive terms given by

$$V_R(r_{ij}) \equiv f_{ij}(r_{ij}) \frac{D_{ij}}{S_{ij}-1} \exp[-\sqrt{2S_{ij}}\beta_{ij}(r-r_0)], \tag{3a}$$

$$V_A(r_{ij}) \equiv f_{ij}(r_{ij}) \frac{S_{ij}D_{ij}}{S_{ij}-1} \exp[-\sqrt{2/S_{ij}}\beta_{ij}(r-r_0)]. \tag{3b}$$

Here $S_{ij}=1.29$, $D_{ij}=6.325\text{eV}$, $\beta_{ij}=15\text{nm}^{-1}$, $r_0=0.1315\text{nm}$, f_{ij}, D_{ij}, S_{ij}, β_{ij} are scalars, $f_{ij}(r_{ij})$ is a switch function used to confine the pair potential in a neighborhood with radius of r_2 as following

$$f_{ij}(r_{ij}) \equiv \begin{cases} 1, & r_{ij} < r_1, \\ \frac{1}{2}\left[1+\cos\left(\frac{\pi(r_{ij}-r_1)}{r_2-r_1}\right)\right], & r_1 \le r_{ij} \le r_2, \\ 0, & r_{ij} > r_2, \end{cases} \tag{3c}$$

where $r_1 = 1.7\,\text{Å}$, $r_2 = 2.0\,\text{Å}$. In Equation (2), $\overline{B}_{ij}$ reads

$$\overline{B}_{ij} \equiv \frac{1}{2}(b_{ij} + b_{ji}), \tag{3d}$$

$$b_{ij} \equiv [1 + \sum_{k \neq i,j} G(\theta_{jik}) f_{ik}(r_{ik})]^{-\delta}, \qquad b_{ji} \equiv [1 + \sum_{k \neq i,j} G(\theta_{ijk}) f_{jk}(r_{jk})]^{-\delta}, \tag{3e}$$

$$G(\theta_{ijk}) \equiv a_0[1 + \frac{c_0^2}{d_0^2} - \frac{c_0^2}{d_0^2 + (1 + \cos\theta_{ijk})^2}], \tag{3f}$$

where θ_{ijk} is the angle between bonds *i-j* and *i-k*, δ = 0.80469, a_0 = 0.011304, $c_0 = 19$ and $d_0 = 2.5$. In addition, the C-C bond length in the model is 0.142nm.

The Verlet algorithm in the velocity form (Leach, 1996) with time step 1 fs is used to simulate the atoms of carbon nanotubes.

$$\begin{aligned} R(t + \delta t) &= R(t) + \delta t V(t) + \frac{1}{2}\delta t^2 a(t) \\ V(t + \delta t) &= V(t) + \frac{1}{2}\delta t[a(t) + a(t + \delta t)] \end{aligned} \tag{4}$$

where, R represents the position, V is the velocity, a denotes the acceleration of atoms, δt is the time step.

3. Flexural wave in a single-walled carbon nanotube

3.1 Non-local elastic Timoshenko beam model

This section starts with the dynamic equation of a non-local elastic Timoshenko beam of infinite length and uniform cross section placed along direction x in the frame of coordinates (x, y, z), with $w(x,t)$ being the displacement of section x of the beam in direction y at the moment t.

In order to describe the effect of microstructure of carbon nanotubes on their mechanical properties, it is assumed that the beam of concern is made of the non-local elastic material, where the stress state at a given reference point depends not only on the strain of this point, but also on the higher-order gradient of strain so as to take the influence of microstructure into account. The simplest constitutive law to characterize the non-local elastic material in the one-dimensional case reads

$$\sigma_x = E(\varepsilon_x + r^2 \frac{\partial^2 \varepsilon_x}{\partial x^2}), \tag{5}$$

where E represents Young's modulus, and ε_x the axial strain. As studied in Askes *et al.* (2002), r is a material parameter to reflect the influence of the microstructure on the stress in the non-local elastic material and yields

$$r = \frac{d}{\sqrt{12}}, \tag{6}$$

where d, referred to as the inter-particle distance, is the axial distance between two rings of particles in the material. For the armchair single-walled carbon nanotube, d is just the axial distance between two rings of carbon atoms.

To establish the dynamic equation of the beam, it is necessary to determine the bending moment M, which reads

$$M = \int_A y\sigma_x \mathrm{d}A, \tag{7}$$

where A represents the cross section area of the beam, σ_x the axial stress, y the distance from the centerline of the cross section. It is well known from the theory of beams that the axial strain yields

$$\varepsilon_x = \frac{y}{\rho'}, \tag{8}$$

where ρ' is the radius of curvature of beam. Let φ denote the slope of the deflection curve when the shearing force is neglected and s denote the coordinate along the deflection curve of the beam, then the assumption upon the small deflection of beam gives

$$\frac{1}{\rho'} = \frac{\partial\varphi}{\partial x}\frac{\partial x}{\partial s} \approx \frac{\partial\varphi}{\partial x}. \tag{9}$$

Substituting Equations (8) and (9) into Equations (5) and (7) gives the following relation between bending moment M and the curvature and its second derivative when the shearing force is neglected

$$M = EI\left(\frac{\partial\varphi}{\partial x} + r^2\frac{\partial^3\varphi}{\partial x^3}\right), \tag{10}$$

where $I = \int y^2 \mathrm{d}A$ represents the moment of inertia for the cross section.

To determine the shear force on the beam, let γ be the angle of shear at the neutral axial in the same cross section. Then, it is easy to see the total slope

$$\frac{\partial w}{\partial x} = \varphi - \gamma. \tag{11}$$

For the torsional problem of one dimension, the constitutive law of the non-local elastic material reads

$$\tau = G\left(\gamma + r^2\frac{\partial^2\gamma}{\partial x^2}\right), \tag{12}$$

where τ is the shear stress and G is the shear modulus. Then, the shear force Q on the cross section becomes

$$Q = \beta AG\left[\left(\varphi - \frac{\partial w}{\partial x}\right) + r^2\left(\frac{\partial^2\varphi}{\partial x^2} - \frac{\partial^3 w}{\partial x^3}\right)\right], \tag{13}$$

where β is the form factor of shear depending on the shape of the cross section, and β =0.5 holds for the circular tube of the thin wall (Timoshenko & Gere, 1972).
Now, it is straightforward to write out the dynamic equation for the beam element of length dx subject to bending M and shear force Q as following

$$\begin{cases} \rho A \dfrac{\partial^2 w}{\partial t^2} \mathrm{d}x + \dfrac{\partial Q}{\partial x} \mathrm{d}x = 0, \\ \rho I \dfrac{\partial^2 \varphi}{\partial t^2} \mathrm{d}x + Q \mathrm{d}x - \dfrac{\partial M}{\partial x} \mathrm{d}x = 0. \end{cases} \tag{14}$$

Substituting Equations (10) and (13) into Equation (14) yields the following coupled dynamic equation for the deflection and the slop of non-local elastic Timoshenko beam

$$\begin{cases} \rho \dfrac{\partial^2 w}{\partial t^2} + \beta G[(\dfrac{\partial \varphi}{\partial x} - \dfrac{\partial^2 w}{\partial x^2}) + r^2 (\dfrac{\partial^3 \varphi}{\partial x^3} - \dfrac{\partial^4 w}{\partial x^4})] = 0, \\ \rho I \dfrac{\partial^2 \varphi}{\partial t^2} + \beta AG[(\varphi - \dfrac{\partial w}{\partial x}) + r^2 (\dfrac{\partial^2 \varphi}{\partial x^2} - \dfrac{\partial^3 w}{\partial x^3})] - EI(\dfrac{\partial^2 \varphi}{\partial x^2} + r^2 \dfrac{\partial^4 \varphi}{\partial x^4}) = 0. \end{cases} \tag{15}$$

3.2 Flexural wave dispersion in different beam models

To study the flexural wave propagation in an infinitely long beam, let the dynamic deflection and slope be given by

$$w(x,t) = \hat{w} \mathrm{e}^{\mathrm{i}\tilde{k}(x-ct)}, \quad \varphi(x,t) = \hat{\varphi} \mathrm{e}^{\mathrm{i}\tilde{k}(x-ct)}, \tag{16}$$

where $\mathrm{i} \equiv \sqrt{-1}$, $\hat{w}$ represents the amplitude of deflection of the beam, and $\hat{\varphi}$ the amplitude of the slope of the beam due to bending deformation alone. In addition, c is the phase velocity of wave, and $\tilde{k}$ is the wave number related to the wave length λ via $\lambda \tilde{k} = 2\pi$. Substituting Equation (16) into Equation (15) yields

$$\begin{cases} (-\mathrm{i}\beta AG\tilde{k} + \mathrm{i}\beta AGr^2\tilde{k}^3)\hat{w} + (-\rho I\tilde{k}^2 c^2 + \beta AG - \beta AGr^2\tilde{k}^2 + EI\tilde{k}^2 - EIr^2\tilde{k}^4)\hat{\varphi} = 0, \\ (-\rho\tilde{k}^2 c^2 + \beta G\tilde{k}^2 - \beta Gr^2\tilde{k}^4)\hat{w} + (\mathrm{i}\beta G\tilde{k} - \mathrm{i}\beta Gr^2\tilde{k}^3)\hat{\varphi} = 0. \end{cases} \tag{17}$$

From the fact that there exists at least one non-zero solution $(\hat{w}, \hat{\varphi})$ of Equation (17), one arrives at

$$\frac{\rho^2 I}{\beta G}\tilde{k}^2 c^4 - [\rho A + \rho I(1 + \frac{E}{\beta G})\tilde{k}^2](1 - r^2\tilde{k}^2)c^2 + EI\tilde{k}^2(1 - r^2\tilde{k}^2)^2 = 0. \tag{18}$$

Solving Equation (18) for the phase velocity c gives two branches of wave dispersion relation

$$c = \sqrt{\frac{-b_1 \pm \sqrt{b_1^2 - 4a_1 c_1}}{2a_1}}, \tag{19}$$

where $a_1 = \rho^2 I\tilde{k}^2 / \beta G$, $b_1 = [\rho A + \rho I(1 + E/\beta G)\tilde{k}^2](r^2\tilde{k}^2 - 1)$ and $c_1 = EI\tilde{k}^2(1 - r^2\tilde{k}^2)^2$. Here, the lower branch represents the dispersion relation of the flexural wave, and the upper branch determines the dispersion relation of the transverse shearing out of interest.

If $r = 0$, Equation (15) leads to

$$\rho A\frac{\partial^2 w(x,t)}{\partial t^2}+EI\frac{\partial^4 w(x,t)}{\partial x^4}-\rho I(1+\frac{E}{\beta G})\frac{\partial^4 w(x,t)}{\partial x^2\partial t^2}+\frac{\rho^2 I}{\beta G}\frac{\partial^4 w(x,t)}{\partial t^4}=0 . \tag{20}$$

This is the dynamic equation of a traditional Timoshenko beam (Timoshenko & Gere, 1972). In this case, the relation of wave dispersion takes the form of Equation (19), but with $a_1 = \rho^2 I\tilde{k}^2 / \beta G$, $b_1 = -[\rho A + \rho I(1 + E / \beta G)\tilde{k}^2]$ and $c_1 = EI\tilde{k}^2$.

If neither the rotary inertial nor the shear deformation is taken into account, Equation (15) leads to the dynamic equation of a non-local elastic Euler beam as following

$$\rho A\frac{\partial^2 w(x,t)}{\partial t^2}+EI[\frac{\partial^4 w(x,t)}{\partial x^4}+r^2\frac{\partial^6 w(x,t)}{\partial x^6}]=0 . \tag{21}$$

The condition of non-zero solution $\hat{w}$ of Equation (21) gives the dispersion relation

$$c=k\sqrt{\frac{EI}{\rho A}(1-r^2\tilde{k}^2)} . \tag{22}$$

In this case, $r = 0$ results in the dispersion relation in the traditional Euler beam

$$c = k\sqrt{\frac{EI}{\rho A}} . \tag{23}$$

When $\tilde{k}^2 < 1/r^2$, there implies a cut off frequency in Equations (19) and (22).

3.3 Flexural wave propagation in a single-walled carbon nanotube

To predict the flexural wave dispersion from the theoretical results in Section 3.2, it is necessary to know Young's modulus *E* and the shear modulus *G* , or Poisson's ratio υ . The previous studies based on the Tersoff-Brenner potential gave a great variety of Young's moduli of single-walled carbon nanotubes from the simulated tests of axial tension and compression. When the thickness of wall was chosen as 0.34nm, for example, 1.07TPa was reported by Yakobson *et al* (1996), 0.8TPa by Cornwell and Wille (1997), and 0.44-0.50TPa by Halicioglu (1998). Meanwhile, the Young's modulus determined by Zhang *et al*. (2002) on the basis of the nano-scale continuum mechanics was only 0.475 TPa when the first set of parameters in the Tersoff-Brenner potential (Brenner, 1990) was used. Hence, it becomes necessary to compute Young's modules and Poisson's ratio again from the above molecular dynamics model for the single-walled carbon nanotubes under the static loading.

For the same thickness of wall, the Young's modulus that we computed by using the first set of parameters in the Tersoff-Brenner potential (Brenner, 1990) was 0.46TPa for the armchair (5,5) carbon nanotube and 0.47TPa for the armchair (10,10) carbon nanotube from the molecular dynamics simulation for the text of axial tension. Furthermore, the simulated test of pure bending that we did gave the product of effective Young's modulus $E = 0.39$TPa and Poisson's ratio $\upsilon = 0.22$ for the armchair (5,5) carbon nanotube, $E = 0.45$TPa and $\upsilon = 0.20$ for the armchair (10,10) carbon nanotube. Young's moduli and Poisson's ratios obtained from the simulated test of pure bending for those two carbon nanotubes were

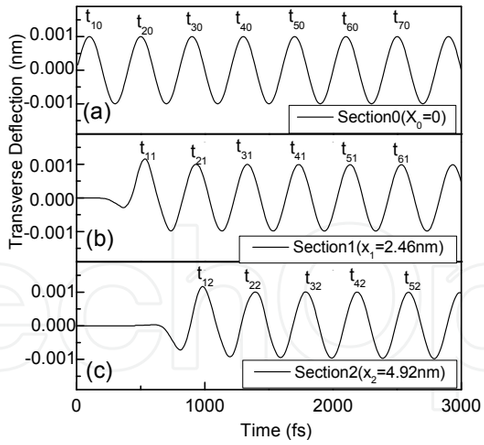

Fig. 2. Time histories of the deflection of different sections of the armchair (5,5) carbon nanotube, where subscripts *i* and *j* in t_{ij} represent the number of wave peak and the number of section, respectively. (a) The sinusoidal wave of period $T = 400\text{fs}$ input at Section 0. (b) The deflection of Section 1, 2.46nm ahead of Section 0. (c) The deflection of Section 2, 4.92nm ahead of Section 0. (Wang & Hu, 2005)

used. In addition, Equation (6) gives $r = 0.0355\text{nm}$ when the axial distance between two rings of atoms reads $d = 0.123\text{nm}$. For the single-walled carbon nanotubes, the wall thickness is $h = 0.34\text{nm}$ and the mass density of the carbon nanotubes is $\rho = 2237\text{kg/m}^3$.

It is quite straightforward to determine the phase velocity and the wave number from the flexural vibration, simulated by using molecular dynamics, of two arbitrary sections of a carbon nanotube. As an example, the end atoms denoted by Section 0 at $x_0 = 0$ of the armchair (5,5) carbon nanotube was assumed to be subject to the harmonic deflection of period $T = 400\text{fs}$ as shown in Figure 2(a). The corresponding angular frequency is $\omega = 2\pi/T \approx 1.57 \times 10^{13}\text{rad/s}$. The harmonic deflection was achieved by shifting the edge atoms of one end of the nanotube while the other end was kept free. Figures 2(b) and 2(c) show the flexural vibrations of Section 1 at $x_1 = 2.46\text{nm}$ and Section 2 at $x_2 = 4.92\text{nm}$, respectively, of the carbon nanotube simulated by using molecular dynamics. If the transient deflection of the first two periods is neglected, the propagation duration Δt of the wave from Section 1 to Section 2 can be estimated as below

$$\Delta t \approx \frac{(t_{32} - t_{31}) + (t_{42} - t_{41}) + \cdots + (t_{n2} - t_{n1})}{n-2}. \tag{24}$$

There follow the phase velocity and wave number

$$c = \frac{x_2 - x_1}{\Delta t}, \quad \tilde{k} = \frac{2\pi}{\lambda} = \frac{\omega T}{\lambda} = \frac{\omega}{c}. \tag{25}$$

Figure 3 illustrate the dispersion relations between the phase velocity c and the wave number of flexural wave in the armchair (5,5) and (10,10) carbon nanotubes, respectively. Here, the symbol E represents the traditional Euler beam, T the traditional Timoshenko beam, NE the non-local elastic Euler beam, NT the non-local elastic Timoshenko beam, and MD the molecular dynamics simulation, respectively. In Figures 3, when the wave number

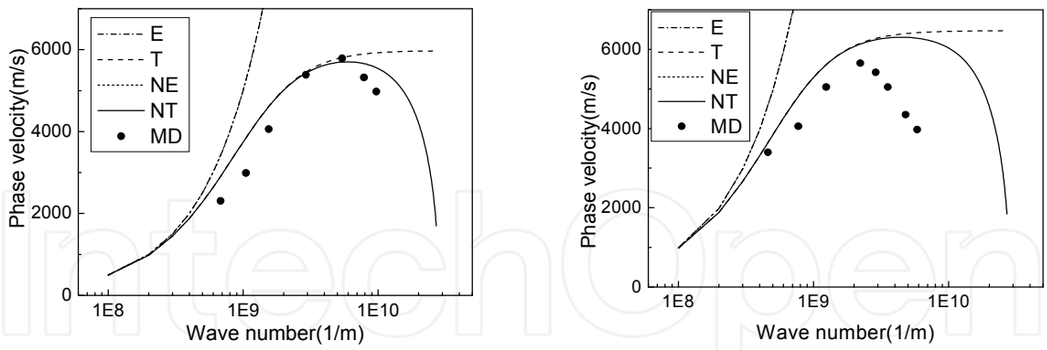

(a) an armchair (5,5) carbon nanotube (b) an armchair (10,10) carbon nanotube

Fig. 3. Dispersion relation of longitudinal wave in single-walled carbon nanotubes. (Wang & Hu, 2005)

$\tilde{k}$ is smaller than $1\times10^{9}m^{-1}$, or the wave length is $\lambda > 6.28\times10^{-9}$m, the phase velocities given by the four beam models are close to each other, and they all could predict the result of the molecular dynamics well. The phase velocity given by the traditional Euler beam, however, is proportional to the wave number, and greatly deviated from the result of molecular dynamics when the wave number became larger than $1\times10^{9}m^{-1}$. Almost not better than the traditional Euler beam, the result of the non-local elastic Euler beam greatly deviate from the result of molecular dynamics too when the wave number became large. Nevertheless, the results of both traditional Timoshenko beam and non-local elastic Timoshenko beam remain in a reasonable coincidence with the results of molecular dynamics in the middle range of wave number or wave length. When the wave number $\tilde{k}$ is larger than $6\times10^{9}\mathrm{m}^{-1}$ (or the wave length is $\lambda < 1.047\times10^{-9}$m) for the armchair (5,5) carbon nanotube and $3\times10^{9}\mathrm{m}^{-1}$ (or the wave length is $\lambda < 2.094\times10^{-9}$m) for the armchair (10,10) carbon nanotube, the phase velocity given by the molecular dynamics begin to decrease, which the traditional Timoshenko beam failed to predict. However, the non-local elastic Timoshenko beam is able to predict the decrease of phase velocity when the wave number is so large (or the wave length was so short) that the microstructure of carbon nanotube significantly block the propagation of flexural waves.

3.4 Group velocity of flexural wave in a single-walled carbon nanotube

The concept of group velocity may be useful in understanding the dynamics of carbon nanotubes since it is related to the energy transportation.

From Equation (19), with $\omega = c\tilde{k}$ considered, the angular frequency ω gives two branches of the wave dispersion relation (Wang *et al*. 2008)

$$\omega = \sqrt{\frac{-b_1 \pm \sqrt{b_1^2 - 4a_1c_1}}{2a_1}}, \tag{26}$$

where $a_1 = \rho^2 I/\beta G$, $b_1 = [-\rho A - \rho I(1+E/\beta G)\tilde{k}^2](1-r^2\tilde{k}^2)$ and $c_1 = EI\tilde{k}^4(1-r^2\tilde{k}^2)^2$. The group velocity reads

$$c_g = \frac{\mathrm{d}\omega}{\mathrm{d}\tilde{k}} = \frac{1}{2\omega}\left(\frac{-\frac{\mathrm{d}b_1}{\mathrm{d}\tilde{k}} \pm (b_1 \frac{\mathrm{d}b_1}{\mathrm{d}\tilde{k}} - 2a_1 \frac{\mathrm{d}c_1}{\mathrm{d}\tilde{k}})\left(b_1^2 - 4a_1c_1\right)^{-1/2}}{2a_1} \right), \tag{27}$$

where

$$\frac{\mathrm{d}b_1}{\mathrm{d}k} = -2\tilde{k}\rho I(1 + E/\beta G)(1 - r^2\tilde{k}^2) - 2r^2\tilde{k}(-\rho A - \rho I(1 + E/\beta G)\tilde{k}^2), \tag{28}$$

$$\frac{\mathrm{d}c_1}{\mathrm{d}k} = 4EI\tilde{k}^3(1 - r^2\tilde{k}^2)^2 - 4EIr^2\tilde{k}^5(1 - r^2\tilde{k}^2). \tag{29}$$

Figure 4 shows the dispersion relations between the group velocity and the wave number of flexural waves in an armchair (5,5) single-walled carbon nanotube and in an armchair (10,10) single-walled carbon nanotube. Here the results were not compared with molecular dynamics results, the Young's modulus used the common value. The product of Young's modulus and the wall thickness is $Eh = 346.8\mathrm{Pa}\cdot\mathrm{m}$ and Poisson's ratio is $\upsilon = 0.20$. There follows $G = E/(2(1+\upsilon))$. In addition, the material parameter $r = 0.0355\mathrm{nm}$. The product of the mass density and the wall thickness yields $\rho h \approx 760.5\mathrm{kg/m}^3\cdot\mathrm{nm}$. For the (5,5) single-walled carbon nanotube, the product of the mass density and the section area yields $\rho A = 1.625\times10^{-15}\mathrm{kg/m}$, the product of the mass density and the moment of inertia for the cross section yields $\rho I = 3.736\times10^{-35}\mathrm{kg}\cdot\mathrm{m}$, and there follows $EI = 1.704\times10^{-26}\mathrm{Pa}\cdot\mathrm{m}^4$. For the (10,10) single-walled carbon nanotube, the product of the mass density and the section area yields $\rho A = 3.25\times10^{-15}\mathrm{kg/m}$, the product of the mass density and the moment of inertia for the cross section yields $\rho I = 2.541\times10^{-34}\mathrm{kg}\cdot\mathrm{m}$, and there follows $EI = 1.159\times10^{-25}\mathrm{Pa}\cdot\mathrm{m}^4$. For both lower and upper branches of the dispersion relation, the results of the elastic Timoshenko beam remarkably deviate from those of the non-local elastic Timoshenko beam with an increase in the wave number. Figure 4(a) and (b) show again the intrinsic limit of the wave number $\tilde{k} < 2\times10^{10}\ \mathrm{m}^{-1}$, instead of $\tilde{k} < \sqrt{12}/d \approx 2.82\times10^{10}\mathrm{m}^{-1}$. This fact explains the difficulty that the cut-off flexural wave predicted by the non-local elastic cylindrical shell is $\tilde{k} < \sqrt{12}/d \approx 2.82\times10^{10}\mathrm{m}^{-1}$, but the direct molecular dynamics simulation only gives the dispersion relation up to the wave number $\tilde{k} \approx 2\times10^{10}\ \mathrm{m}^{-1}$ (Wang & Hu, 2005).

4. Longitudinal wave in a single-walled carbon nanotube

4.1 Wave dispersion predicted by a non-local elastic shell model

This section studies the dispersion of longitudinal waves from a thoughtful model, namely, the model of a cylindrical shell made of non-local elastic material. For such a thin cylindrical shell, the bending moments can be naturally neglected for simplicity in theory. Figure 5(a) shows a shell strip cut from the cylindrical shell, where a set of coordinates $(x,\theta,\tilde{r})$ is defined, and Figure 5(b) gives the forces on the shell strip of unit length when the bending moments are negligible (Graff 1975). The dynamic equations of the cylindrical shell in the longitudinal, tangential, and radial directions $(x,\theta,\tilde{r})$ read

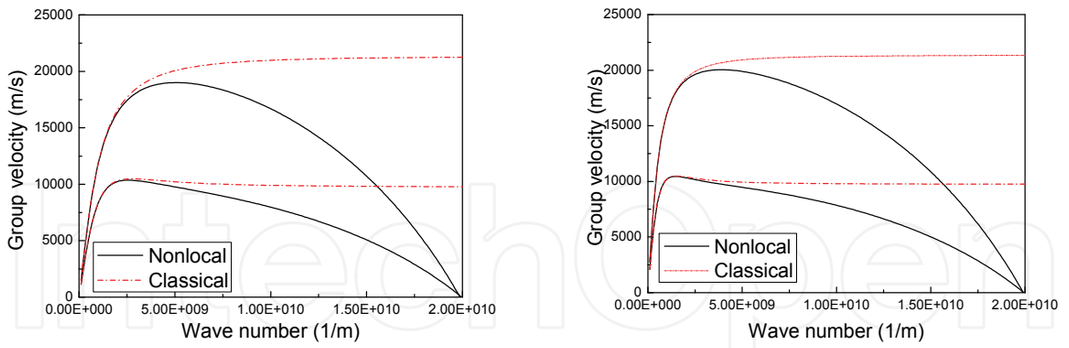

(a) an armchair (5,5) carbon nanotube (b) an armchair (10,10) carbon nanotube

Fig. 4. Dispersion relations between the group velocity and the wave number of flexural waves in single-walled carbon nanotubes (Wang *et al*. 2008a)

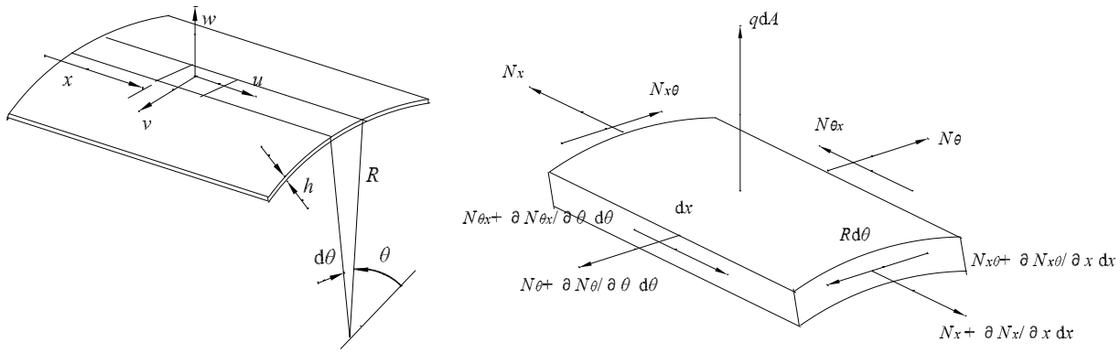

(a) (b)

Fig. 5. The model of a cylindrical shell made of non-local elastic material
(a) A strip from the cylindrical shell,
(b) A small shell element and the internal forces (Wang *et al*. 2006b)

$$\rho h\frac{\partial^2 u}{\partial t^2}-\frac{\partial N_x}{\partial x}-\frac{1}{R}\frac{\partial N_{\theta x}}{\partial \theta}=0\,, \tag{30a}$$

$$\rho h\frac{\partial^2 v}{\partial t^2}-\frac{1}{R}\frac{\partial N_\theta}{\partial \theta}-\frac{\partial N_{x\theta}}{\partial x}=0\,, \tag{30b}$$

$$\rho h\frac{\partial^2 w}{\partial t^2}+\frac{N_\theta}{R}=0\,, \tag{30c}$$

where h presents the thickness of the shell, R the radius of the shell, ρ the mass density, (u,v,w) the displacement components $(x,\theta,\tilde{r})$. $N_x, N_\theta, N_{x\theta}, N_{\theta x}$, the components of the internal force in the shell, can be determined by integrating the corresponding stress components $\sigma_x, \sigma_\theta, \tau_{x\theta}, \tau_{\theta x}$ across the shell thickness as following

$$N_x, N_\theta, N_{x\theta}, N_{\theta x} = \int_{-h/2}^{h/2} (\sigma_x, \sigma_\theta, \tau_{x\theta}, \tau_{\theta x}) \mathrm{d}z \,, \tag{31}$$

where z is measured outward from the mid surface of the shell.
The constitutive law of the two-dimensional non-local elastic continuum for the cylindrical shell under the load of axial symmetry as follows,

$$\sigma_x = \lambda(\varepsilon_x + \varepsilon_\theta) + 2\mu\varepsilon_x + \lambda(r_x^2 \frac{\partial^2 \varepsilon_x}{\partial x^2} + r_x^2 \frac{\partial^2 \varepsilon_\theta}{\partial x^2}) + 2\mu r_x^2 \frac{\partial^2 \varepsilon_x}{\partial x^2} \,, \tag{32a}$$

$$\sigma_\theta = \lambda(\varepsilon_x + \varepsilon_\theta) + 2\mu\varepsilon_\theta + \lambda(r_x^2 \frac{\partial^2 \varepsilon_x}{\partial x^2} + r_x^2 \frac{\partial^2 \varepsilon_\theta}{\partial x^2}) + 2\mu r_x^2 \frac{\partial^2 \varepsilon_\theta}{\partial x^2} \,, \tag{32b}$$

$$\tau_{x\theta} = 2\mu\varepsilon_{x\theta} + 2\mu r_x^2 \frac{\partial^2 \varepsilon_{x\theta}}{\partial x^2} \,. \tag{32c}$$

Let $\gamma = 2\varepsilon_{x\theta}$ and γ be the shear strain of the element with $\gamma = \gamma_{x\theta} = \gamma_{\theta x}$. Substituting $\mu = E/(2+2\upsilon) = G$ and $\lambda = E\upsilon/(1-\upsilon^2)$ into Equation (32) yields

$$\sigma_x = \frac{E}{1-\upsilon^2}[\varepsilon_x + r_x^{\,2} \frac{\partial^2 \varepsilon_x}{\partial x^2} + \upsilon(\varepsilon_\theta + r_x^{\,2} \frac{\partial^2 \varepsilon_\theta}{\partial x^2})] \,, \tag{33a}$$

$$\sigma_\theta = \frac{E}{1-\upsilon^2}[\varepsilon_\theta + r_x^2 \frac{\partial^2 \varepsilon_\theta}{\partial x^2} + \upsilon(\varepsilon_x + r_x^{\,2} \frac{\partial^2 \varepsilon_x}{\partial x^2})] \,, \tag{33b}$$

$$\tau_{x\theta} = \tau_{\theta x} = G(\gamma + r_x^{\,2} \frac{\partial \gamma^2}{\partial x^2}) \,, \tag{33c}$$

where $r_x = r = d/\sqrt{12}$ characterizes the influence of microstructures on the constitutive law of the non-local elastic materials, and d, referred to as the inter-particle distance (Askes et al, 2002), is the axial distance between rings of carbon atoms when a single walled carbon nanotube is modeled as a non-local elastic cylindrical shell.
Under the assumption that only the membrane stresses play a role in the thin cylindrical shells, the stress components $\sigma_x, \sigma_\theta, \tau_{x\theta}, \tau_{\theta x}$ are constants throughout the shell thickness such that Equation (31) yields

$$N_x = \frac{Eh}{1-\upsilon^2}[\varepsilon_x + r^2 \frac{\partial^2 \varepsilon_x}{\partial x^2} + \upsilon(\varepsilon_\theta + r^2 \frac{\partial^2 \varepsilon_\theta}{\partial x^2})] \,, \tag{34a}$$

$$N_\theta = \frac{Eh}{1-\upsilon^2}[\varepsilon_\theta + r^2 \frac{\partial^2 \varepsilon_\theta}{\partial x^2} + \upsilon(\varepsilon_x + r^2 \frac{\partial^2 \varepsilon_x}{\partial x^2})] \,, \tag{34b}$$

$$N_{x\theta} = N_{\theta x} = Gh(\gamma + r \frac{\partial \gamma^2}{\partial r^2}) = \frac{Eh}{2(1+\upsilon)}(\gamma + r^2 \frac{\partial \gamma^2}{\partial x^2}) \,. \tag{34c}$$

The geometric relation under the condition $\partial/\partial\theta = 0$ leads to $\varepsilon_x = \partial u/\partial x$, $\varepsilon_\theta = w/R$, $\gamma = \partial v/\partial x$. Substituting Equation (34) into Equation (30) gives a set of dynamic equations of the non-local elastic cylindrical shell

$$\frac{\rho(1-\upsilon^2)}{E}\frac{\partial^2 u}{\partial t^2}-\frac{\partial^2 u}{\partial x^2}-r^2\frac{\partial^4 u}{\partial x^4}-\frac{\upsilon}{R}(\frac{\partial w}{\partial x}+r^2\frac{\partial^3 w}{\partial x^3})=0, \tag{35a}$$

$$\frac{2\rho(1+\upsilon)}{E}\frac{\partial v^2}{\partial t^2}-\frac{\partial^2 v}{\partial x^2}-r^2\frac{\partial^4 v}{\partial x^4}=0\,, \tag{35b}$$

$$\frac{\rho(1-\upsilon^2)}{E}\frac{\partial^2 w}{\partial t^2}+\frac{1}{R^2}(w+r^2\frac{\partial^2 w}{\partial x^2})+\frac{\upsilon}{R}(\frac{\partial u}{\partial x}+r^2\frac{\partial^3 u}{\partial x^3})=0\,. \tag{35c}$$

Obviously, Equation (35b) is not coupled with Equations (35a) and (35c) such that the torsional wave in the cylindrical shell is independent of the longitudinal and radial waves. Now consider the motions governed by the coupled dynamic equations in u and w. Let

$$u=\hat{u}\mathrm{e}^{\mathrm{i}\tilde{k}(x-ct)}\,,\ w=\hat{w}\mathrm{e}^{\mathrm{i}\tilde{k}(x-ct)} \tag{36}$$

where $\mathrm{i}\equiv\sqrt{-1}$, $\hat{u}$ is the amplitude of longitudinal vibration, $\hat{w}$ the amplitude of radial vibration. c and $\tilde{k}$ are the same as previous definition. Substituting Equation (36) into Equations (35a) and (35c) yields

$$\begin{bmatrix}\frac{\tilde{k}^2c^2}{c_p^2}-\tilde{k}^2+r^2\tilde{k}^4 & \mathrm{i}(\tilde{k}-r^2\tilde{k}^3)\frac{\upsilon}{R}\\ -\mathrm{i}(\tilde{k}-r^2\tilde{k}^3)\frac{\upsilon}{R} & \frac{\tilde{k}^2c^2}{c_p^2}-\frac{1}{R^2}(1-r^2\tilde{k}^2)\end{bmatrix}\begin{bmatrix}\hat{u}\\ \hat{w}\end{bmatrix}=0\,. \tag{37}$$

where $c_p\equiv\sqrt{E/((1-\upsilon^2)\rho)}$, which is usually referred to as 'thin-plate' velocity. The existence of non-zero solution $[\hat{u}\ \ \hat{w}]^{\mathrm{T}}$ of Equation (37) requires

$$c^4-c_p^2(1+\frac{1}{R^2\tilde{k}^2})(1-r^2\tilde{k}^2)c^2+\frac{c_p^4(1-\upsilon^2)}{R^2\tilde{k}^2}(1-r^2\tilde{k}^2)^2=0\,. \tag{38}$$

Solving Equation (38) for the dimensionless phase velocity c/c_p gives the two branches of the wave dispersion relation as following

$$\frac{c}{c_p}=\sqrt{\frac{(1+\frac{1}{R^2\tilde{k}^2})\mp\sqrt{(1+\frac{1}{R^2\tilde{k}^2})^2-4\frac{1-\upsilon^2}{R^2\tilde{k}^2}}}{2}(1-r^2\tilde{k}^2)}\,. \tag{39}$$

Equation (39) shows again the intrinsic limit $1-r^2\tilde{k}^2>0$ or $\tilde{k}<\sqrt{12}/d$ for the maximal wave number owing to the microstructure. That is, the longitudinal wave is not able to propagate in the non-local elastic cylindrical shell if the wave length is so short that $\lambda<\pi d/\sqrt{3}\approx 1.814d$ holds. If $r=0$ in Equation (39), one arrives at

$$\frac{c}{c_p}=\sqrt{\frac{(1+\frac{1}{R^2\tilde{k}^2})\mp\sqrt{(1+\frac{1}{R^2\tilde{k}^2})^2-4\frac{1-\upsilon^2}{R^2\tilde{k}^2}}}{2}}\,. \tag{40}$$

This is just the wave dispersion relation of the traditional elastic cylindrical shell.

4.2 Wave propagation simulated by molecular dynamics

This section presents the longitudinal wave dispersion from the theoretical results in Section 4.1 compared with the molecular dynamics results for the longitudinal wave propagation in an armchair (5,5) carbon nanotube and an armchair (10,10) carbon nanotube, respectively, for a wide range of wave numbers.

In the molecular dynamics models, the interatomic interactions are also described by the Tersoff-Brenner potential (Brenner, 1990). It is quite straightforward to determine the phase velocity and the wave number from the longitudinal vibration, simulated by using the molecular dynamics model, of two arbitrary sections of the carbon nanotube. The Young's moduls was 0.46TPa for the armchair (5,5) carbon nanotube and 0.47TPa for the armchair (10,10) carbon nanotube from the molecular dynamics simulation for the text of axial tension. Furthermore, Poisson's ratio $\upsilon = 0.22$ for the armchair (5,5) and $\upsilon = 0.20$ for the armchair (10,10) carbon nanotube.

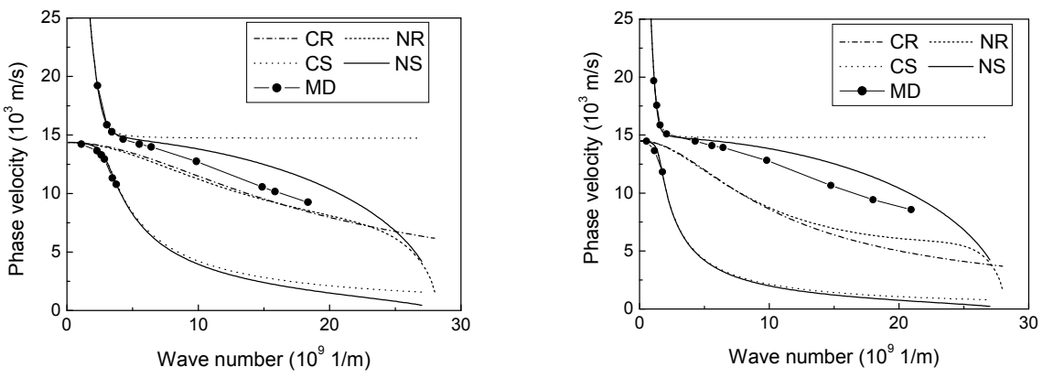

(a) an armchair (5,5) carbon nanotube (b) an armchair (10,10) carbon nanotube.

Fig. 6. The wave dispersion relations between phase velocity versus wave number given by the models of elastic cylindrical shell and non-local elastic cylindrical shell in comparison with molecular dynamics simulations. (Wang *et al*. 2006b)

Figure 6 shows the dispersion relation between the phase velocity c and the wave number $\tilde{k}$, and the dispersion relation between the angular frequency ω and the wave number $\tilde{k}$ given by the models of both elastic cylindrical shell and non-local elastic cylindrical shell in comparison with the numerical simulations of molecular dynamics for the two carbon nanotubes. In Figure 6, the symbol NS represents the model of non-local elastic cylindrical shell as in Equation (40), the symbol CS the model of elastic cylindrical shell as in Equation (41), the symbol CR the rod model of Love theory, the symbol NR the non-local elastic rod model with lateral inertial taken into consideration (Wang, 2005), and MD the molecular dynamics simulation. Obviously, only the results from the model of non-local elastic cylindrical shell coincide well with the two branches of dispersion relations given by molecular dynamics simulations.

4.3 Group velocity of longitudinal wave in a single-walled carbon nanotube

From Equation (39), with $\omega = c\tilde{k}$ considered, the two branches of the wave dispersion relation as following

$$\omega = c_p \sqrt{\frac{(\tilde{k}^2 + \frac{1}{R^2}) \mp \sqrt{(\tilde{k}^2 + \frac{1}{R^2})^2 - 4\frac{(1-\upsilon^2)\tilde{k}^2}{R^2}}}{2}(1 - r^2\tilde{k}^2)} \,. \tag{41}$$

Then, the group velocity reads

$$\begin{aligned} c_g &= \frac{\mathrm{d}\omega}{\mathrm{d}\tilde{k}} \\ &= \frac{c_p}{2\sqrt{2}}\left\{\left(2\tilde{k} \mp \{[2\tilde{k}(\tilde{k}^2 + \frac{1}{R^2})] - 4\tilde{k}\frac{1-\upsilon^2}{R^2}\}[(\tilde{k}^2 + \frac{1}{R^2})^2 - 4\frac{(1-\upsilon^2)\tilde{k}^2}{R^2}]^{-\frac{1}{2}}\right)(1 - r^2\tilde{k}^2)\right. \\ &\left. + \left[(\tilde{k}^2 + \frac{1}{R^2}) \mp \sqrt{(\tilde{k}^2 + \frac{1}{R^2})^2 - 4\frac{(1-\upsilon^2)\tilde{k}^2}{R^2}}\right]\left(-2r^2\tilde{k}\right)\right\} \\ &\left\{\left[(\tilde{k}^2 + \frac{1}{R^2}) \mp \sqrt{(\tilde{k}^2 + \frac{1}{R^2})^2 - 4\frac{(1-\upsilon^2)\tilde{k}^2}{R^2}}\right](1 - r^2\tilde{k}^2)\right\}^{-\frac{1}{2}} . \end{aligned} \tag{42}$$

Figure 7 shows the dispersion relation between the group velocity and the wave number of longitudinal waves in an armchair (5,5) single-walled carbon nanotube and in an armchair (10,10) single-walled carbon nanotube. Now, the product of Young's modulus E and the wall thickness h is $Eh = 346.8\mathrm{Pa}\cdot\mathrm{m}$, and Poisson's ratio is $\upsilon = 0.20$ for the (5,5) single-walled carbon nanotube and the (10,10) single-walled carbon nanotube. In addition, one has $r = 0.0355\mathrm{nm}$ when the axial distance between two neighboring rings of atoms is $d = 0.123\mathrm{nm}$. The product of mass density ρ and the wall thickness h yields $\rho h \approx 760.5$ $\mathrm{kg/m^3}\cdot\mathrm{nm}$. The radii of the (5, 5) and (10, 10) single-walled carbon nanotubes are 0.34nm and 0.68nm, respectively. There is a slight difference between the theory of non-local elasticity and the classical theory of elasticity for the lower branches. The group velocity decreases rapidly with an increase in the wave number. When the wave number approaches to $\tilde{k} = 5\times10^9\ \mathrm{m^{-1}}$ or so, the group velocity goes to zero for the (5,5) single-walled carbon nanotube. Similarly, the group velocity approaches to zero for the (10, 10) single-walled carbon nanotube when the wave number goes to $\tilde{k} = 3\times10^9\ \mathrm{m^{-1}}$ or so. This may explain the difficulty that the direct molecular dynamics simulation can only offer the dispersion relation between the phase velocity and the wave number up to $\tilde{k} \approx 5\times10^9\ \mathrm{m^{-1}}$ for the (5,5) single-walled carbon nanotube and up to $\tilde{k} \approx 3\times10^9\ \mathrm{m^{-1}}$ for the (10,10) single-walled carbon nanotube. For the upper branches of the dispersion relation, the difference can hardly be identified when the wave number is lower. However, the results of the elastic cylindrical shell remarkably deviate from those of the non-local elastic cylindrical shells with an increase in the wave number. Figure 7 (a) and (b) show the intrinsic limit $\tilde{k} < 2\times10^{10}\ \mathrm{m^{-1}}$, instead of $\tilde{k} < \sqrt{12}/d \approx 2.82\times10^{10}\mathrm{m^{-1}}$ for the maximal wave number owing to the micro-structures. This can explain the contradiction that the cut-off longitudinal wave predicted by

the non-local elastic cylindrical shell is $\tilde{k}<\sqrt{12}/d\approx 2.82\times10^{10}\,\mathrm{m}^{-1}$, but the molecular dynamics simulation offers the dispersion relation up to the wave number $\tilde{k}\approx 2\times10^{10}\,\mathrm{m}^{-1}$ only (Wang et al. 2006b).

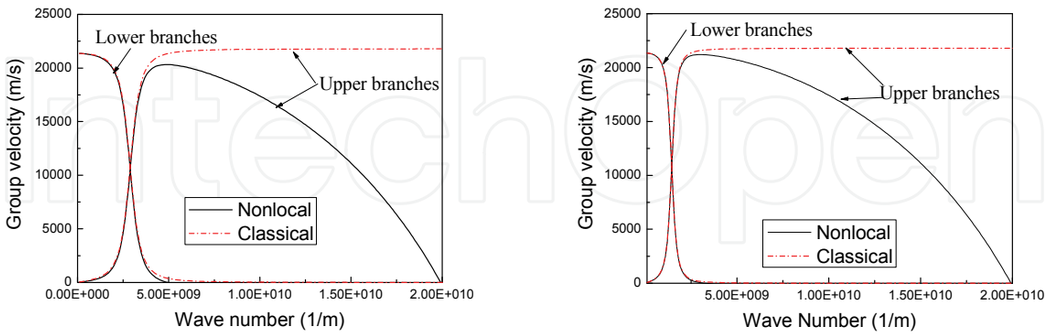

(a) an armchair (5,5) carbon nanotube (b) an armchair (10,10) carbon nanotube

Fig. 7. Dispersion relations between the group velocity and the wave number of longitudinal waves in armchair single-walled carbon nanotubes (Wang *et al*. 2008a)

5. Flexural waves in a multi-walled carbon nanotube

5.1 Multi Timoshenko beam model

Here, a nonlocal multiple-elastic Timoshenko beam model with second order strain gradient taken into consideration is developed, in which each of the nested, originally concentric nanotubes of a multi-walled carbon nanotube is described as an individual elastic beam, and the deflections of all nested tubes are coupled through the van der Waals interaction between any two tubes. Since all nested tubes of a multi-walled carbon nanotube are originally concentric and the van der Waals interaction is determined by the interlayer spacing, the net van der Waals interaction pressure remains zero for each of the tubes provided they deform coaxially. Thus, for small-deflection linear vibration the interaction pressure at any point between any two adjacent tubes linearly depends on the difference of their deflections at that point. Here, we assume that all nested individual tubes of the multi-walled carbon nanotube vibrate in the same plane. Thus, coplanar transverse vibration of N nested tubes of an N wall is described by N coupled equations. The dynamics equations of the j th layer for N-walled carbon nanotube,

$$\rho A_k \frac{\partial^2 w_k}{\partial t^2}+\beta A_k G\left[\left(\frac{\partial \varphi_k}{\partial x}+r^2\frac{\partial^3 \varphi_k}{\partial x^3}\right)-\left(\frac{\partial^2 w_k}{\partial x^2}+r^2\frac{\partial^4 w_k}{\partial x^4}\right)\right]=w_k\sum_{j=1}^{n}C_{kj}-\sum_{j=1}^{n}C_{kj}w_j \tag{43a}$$

$$\rho I_k \frac{\partial^2 \varphi_k}{\partial t^2}+\beta A_k G\left[(\varphi_k-\frac{\partial w_k}{\partial x})+r^2\left(\frac{\partial^2 \varphi_k}{\partial x^2}-\frac{\partial^3 w_k}{\partial x^3}\right)\right]-EI_k(\frac{\partial^2 \varphi_k}{\partial x^2}+r^2\frac{\partial^4 \varphi_k}{\partial x^4})=0 \tag{43b}$$

where E, G, υ, r, ρ, h represents the same meaning as previous sections. A_k represents the cross section area of the beam, $I_k=\int y^2 dA_k$ represents the moment of inertia for the cross section, w_k being the displacement of section, φ_k denote the slope of the deflection curve when the shearing force is neglected.

For small-deflection linear vibration, the van der Waals pressure at any point between two tubes should be a linear function of the jump in deflection at that point.

$$p_k = \sum_{k=1}^{n} C_{kj}(w_k - w_j) = w_k \sum_{j=1}^{n} C_{kj} - \sum_{j=1}^{n} C_{kj} w_j \tag{44}$$

where N is the total number of layers of the multi-walled carbon nanotube. C_{kj} is the van der Waals interaction coefficients for interaction pressure per unit axial length can be estimated based on an effective interaction width (Ru, 2000)

$$C_{kj} = 2R_k c_{kj} \tag{45}$$

The van der Waals interaction coefficients can be obtained through the Lennard-Jones pair potential (Jones, 1924; Girifalco & Lad, 1956)

$$V(r) = 4\varepsilon[(\sigma/\tilde{r})^{12} - (\sigma/\tilde{r})^{6}]\,. \tag{46}$$

where $\varepsilon = 2.968 \times 10^{-3}\text{eV}$, $\sigma = 3.407\,\text{Å}$, where $\tilde{r}$ is the distance between two interacting atoms.

Note that the attractive van der Waals force that is obtained from the Lennard-Jones pair potential is negative, the repulsive van der Waals force is positive, and the downward pressure is assumed to be positive.

Here, van der Waals interaction coefficients c_{jk} obtained through the Lennard-Jones pair potential by He et al. (2005) are used.

$$c_{kj} = -\left[\frac{1001\pi\varepsilon\sigma^{12}}{3a^4}E_{kj}^{13} - \frac{1120\pi\varepsilon\sigma^{6}}{9a^4}E_{kj}^{7}\right]R_j\,, \tag{47}$$

where

$$E_{kj}^{m} = (R_k + R_j)^{-m}\int_0^{\frac{\pi}{2}} \frac{d\theta}{\left[1 - K_{kj}\cos^2\theta\right]^{\frac{m}{2}}}\,, \tag{48}$$

and

$$K_{kj} = \frac{4R_k R_j}{(R_k + R_j)^2}\,. \tag{49}$$

5.2 Dispersion of flexural wave in multi-walled carbon nanotubes

To study the flexural wave propagation, let us consider the deflection and the slope given by

$$w_k = \hat{w}_k e^{\mathrm{i}\tilde{k}(x-ct)}, \quad \varphi_k = \hat{\varphi}_k e^{\mathrm{i}\tilde{k}(x-ct)}, \quad (k = 1\cdots n) \tag{50}$$

where $\mathrm{i} \equiv \sqrt{-1}$, $\hat{w}_k$ represent the amplitudes of deflections of the k th tube, and $\hat{\varphi}_k$ the amplitudes of the slopes of the j th tube due to bending deformation alone. In addition, c and $\tilde{k}$ are the same as previous definition. Substituting Equation (50) into Equation (43) yields

$$\begin{cases} (\rho\tilde{k}^2c^2 - \beta G\tilde{k}^2 + \beta Gr^2\tilde{k}^4)\hat{w}_k - (\mathrm{i}\beta G\tilde{k} - \mathrm{i}\beta Gr^2\tilde{k}^3)\hat{\varphi}_k + \hat{w}_k \sum_{j=1}^{n} C_{kj} \Big/ A_k - \sum_{j=1}^{n} \frac{C_{kj}}{A_k}\hat{w}_j = 0 \\ (\mathrm{i}\beta A_k G\tilde{k} - \mathrm{i}\beta A_k Gr^2\tilde{k}^3)\hat{w}_k + (\rho I_k\tilde{k}^2c^2 - \beta A_k G + \beta A_k Gr^2\tilde{k}^2 - EI_k\tilde{k}^2 + EI_k r^2\tilde{k}^4)\hat{\varphi}_k = 0 \end{cases} \tag{51}$$

From the fact that there exists at least one non-zero solution $(\hat{w},\hat{\varphi})$ of Equation (51), one arrives at

$$\left[\rho\tilde{k}^2c^2\mathbf{I}_{2n\times 2n} + \mathbf{H}_{2n\times 2n}\right]\begin{bmatrix} \hat{w}_1 \\ \hat{\varphi}_1 \\ \hat{w}_2 \\ \hat{\varphi}_2 \\ \vdots \\ \hat{w}_n \\ \hat{\varphi}_n \end{bmatrix} = 0\,, \tag{52}$$

where $\mathbf{I}_{2n\times 2n}$ is an identity matrix and the elements in the matrix $\mathbf{H}_{2n\times 2n}$ are

$$\mathbf{H}(2k-1,2j-1) = -\frac{C_{kj}}{A_k} \quad (j \neq k) \tag{53a}$$

$$\mathbf{H}(2k-1,2k-1) = -\beta G\tilde{k}^2 + \beta Gr^2\tilde{k}^4 + \sum_{j=1}^{n} C_{kj} \Big/ A_k\,; \tag{53b}$$

$$\mathbf{H}(2k-1,2k) = -(\mathrm{i}\beta G\tilde{k} - \mathrm{i}\beta Gr^2\tilde{k}^3)\,; \tag{53c}$$

$$\mathbf{H}(2k,2k-1) = (\mathrm{i}\beta A_k G\tilde{k} - \mathrm{i}\beta A_k Gr^2\tilde{k}^3)/I_k\,; \tag{53d}$$

$$\mathbf{H}(2k,2k) = (-\beta A_k G + \beta A_k Gr^2\tilde{k}^2 - EI_k\tilde{k}^2 + EI_k r^2\tilde{k}^4)/I_k\,; \tag{53e}$$

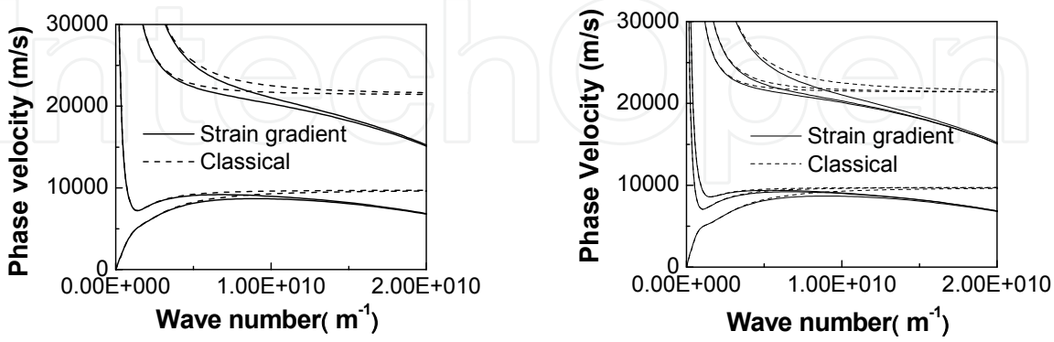

(a) A double-walled carbon nanotube ((5,5),(10,10))

(b) A triple-walled carbon nanotube ((5,5),(10,10),(15,15))

Fig. 8. Flexural wave dispersion of multi-walled carbon nanotubes given by strain gradient Timoshenko model compared with classical Timoshenko model

Figure 8 show the comparison of strain gradient Timoshenko beam model and classical Timoshenko model in deal with the flexural wave dispersion of a double-walled carbon nanotubes ((5,5),(10,10)) and a triple-walled carbon nanotubes ((5,5),(10,10),(15,15)). Where in Equations (52) and (53), Young's modulus $E = 1.02\text{TPa}$, shear modulus $G = E/2(1+\upsilon)$ and poisson ratio $\upsilon = 0.2$, the shear form factor $\beta = 0.5$, the material parameter $r = 0.0355\text{nm}$, the mass density $\rho = 2237\text{kg/m}^3$, thickness $h = 0.34\text{nm}$. In all these figures, it can be seen, the difference of the dispersion relation between phase velocity and wave number given by strain gradient shell model and classical shell model is more and more obviously with the increase of wave number. This is similar as single walled carbon nanotubes' results (Wang & Hu, 2005).

5.3 Group velocity of flexural waves in a multi-walled carbon nanotube

Under the assumption that there exists at least one non-zero solution $(\hat{w}_k, \hat{\varphi}_k)$ of Equation (51), with $\omega = c\tilde{k}$ considered, one arrives at

$$\left[\rho\omega^2\mathbf{I}_{2n\times 2n} + \mathbf{H}_{2n\times 2n}\right]\begin{bmatrix}\hat{w}_1\\ \hat{\varphi}_1\\ \hat{w}_2\\ \hat{\varphi}_2\\ \vdots\\ \hat{w}_n\\ \hat{\varphi}_n\end{bmatrix} = 0\,, \tag{54}$$

where $\mathbf{I}_{2n\times 2n}$ is an identity matrix and the entries in matrix $\mathbf{H}_{2n\times 2n}$ are

$$\mathbf{H}(2k-1, 2j-1) = -\frac{C_{kj}}{A_k} \quad (j \neq k)\,, \tag{55a}$$

$$\mathbf{H}(2k-1, 2k-1) = -\beta G\tilde{k}^2 + \beta G r^2\tilde{k}^4 + \sum_{j=1}^{n} C_{kj} \Big/ A_k\,, \tag{55b}$$

$$\mathbf{H}(2k-1, 2k) = -(\mathrm{i}\beta G\tilde{k} - \mathrm{i}\beta G r^2\tilde{k}^3)\,, \tag{55c}$$

$$\mathbf{H}(2k, 2k-1) = (\mathrm{i}\beta A_k G\tilde{k} - \mathrm{i}\beta A_k G r^2\tilde{k}^3)/I_k\,, \tag{55d}$$

$$\mathbf{H}(2k, 2k) = (-\beta A_k G + \beta A_k G r^2\tilde{k}^2 - EI_k\tilde{k}^2 + EI_k r^2\tilde{k}^4)/I_k\,. \tag{55e}$$

From Equation (54), the dispersion relation between the group velocity and the wave number of flexural waves in a multi-walled carbon nanotube can be numerically obtained by using $c_g = \mathrm{d}\omega/\mathrm{d}\tilde{k}$.

Number of tube k (radius)	ρA_k (kg/m)	ρI_k(kg·m)	EI_k(Pa·m^4)
k=1 (0.34nm)	1.625×10^{-15}	3.737×10^{-35}	1.704×10^{-26}
k=2 (0.68nm)	3.250×10^{-15}	2.541×10^{-34}	1.158×10^{-25}

Table 1. Parameters of a double-wall carbon nanotube

Number of tube k (radius)	ρA_k (kg/m)	ρI_k(kg·m)	EI_k(Pa·m^4)
k=1 (0.34nm)	1.625×10^{-15}	3.737×10^{-35}	1.704×10^{-26}
k=2 (0.68nm)	3.250×10^{-15}	2.541×10^{-34}	1.158×10^{-25}
k=3 (1.02nm)	4.874×10^{-15}	8.296×10^{-34}	3.782×10^{-25}
k=4 (1.36nm)	6.466×10^{-15}	1.943×10^{-33}	8.860×10^{-25}

Table 2. Parameters of a quadruple-wall carbon nanotube

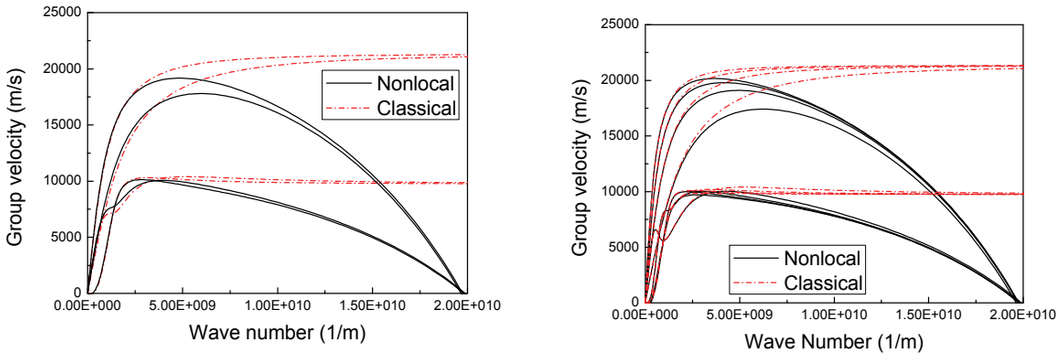

(a) A double-walled carbon nanotube with the radii 0.34nm and 0.68nm.

(b) A quadruple -walled carbon nanotube with the radii 0.34nm, 0.68nm, 1.02nm and 1.36nm

Fig. 9. Dispersion relations between the group velocity and the wave number of flexural wave in multi-walled carbon nanotubes. (Wang *et al*. 2008a)

Figure 9 presents the dispersion relation between the group velocity and the wave number of flexural waves in a double-walled carbon nanotube with the radii $R_1 = 0.34\text{nm}$ and $R_2 = 0.68\text{nm}$ respectively, and in a quadruple-walled carbon nanotube with the radii $R_1 = 0.34\text{nm}$, $R_2 = 0.68\text{nm}$, $R_3 = 1.02\text{nm}$ and $R_4 = 1.36\text{nm}$ respectively. The product of Young's modulus and the wall thickness is $Eh = 346.8\text{Pa}\cdot\text{m}$, and Poisson's ratio is $\upsilon = 0.20$. There follows $G = E/(2(1+\upsilon))$. The product of mass density and the wall thickness yields $\rho h \approx 760.5\text{kg/m}^3\cdot\text{nm}$, and the form factor of shear $\beta = 0.5$. Table 1 shows the parameters $\rho A_k, \rho I_k, EI_k$ of the double-walled carbon nanotube. Table 2 gives the parameters $\rho A_k, \rho I_k, EI_k$ of the quadruple-walled carbon nanotube. For all these lower branches and the upper branches of the dispersion relation, the difference is almost invisible when the wave number is lower. However, the results of the elastic model of Timoshenko beams remarkably deviate from those of non-local elastic model of Timoshenko beams with an increase in the wave number. Figures 9 (a) and (b) show again the intrinsic limit

$\tilde{k} < 2\times10^{10}$ m^{-1}, rather than $\tilde{k} < \sqrt{12}/d \approx 2.82\times10^{10}$ m^{-1} for the maximal wave number owing to the micro-structures.

6. Longitudinal wave in a multi-walled carbon nanotube

6.1 Strain gradient multi shell model

This section studies dispersion of longitudinal wave in a multi-walled carbon nanotube with a multi-cylindrical shell model that takes into consideration the second order strain gradient. For such a thin cylindrical shell, the bending moments can be naturally neglected for simplicity. The dynamics equations of the k th layer for an N-walled carbon nanotube are

$$\frac{\rho(1-\upsilon^2)}{E}\frac{\partial^2 u_k}{\partial t^2} - \frac{\partial^2 u_k}{\partial x^2} - r^2\frac{\partial^4 u_k}{\partial x^4} - \frac{\upsilon}{R_k}\left(\frac{\partial w_k}{\partial x} + r^2\frac{\partial^3 w_k}{\partial x^3}\right) = 0, \tag{56a}$$

$$\frac{2\rho(1+\upsilon)}{E}\frac{\partial^2 v_k}{\partial t^2} - \frac{\partial^2 v_k}{\partial x^2} - r^2\frac{\partial^4 v_k}{\partial x^4} = 0, \tag{56b}$$

$$\frac{\rho(1-\upsilon^2)}{E}\frac{\partial^2 w_k}{\partial t^2} + \frac{1}{R_k{}^2}\left(w_k + r^2\frac{\partial^2 w_k}{\partial x^2}\right) + \frac{\upsilon}{R_k}\left(\frac{\partial u_k}{\partial x} + \frac{\partial^3 u_k}{\partial x^3}\right) = \frac{q_k(1-\upsilon^2)}{Eh}. \tag{56c}$$

As only infinitesimal vibration is considered, the net pressure due to the van der Waals interaction is assumed to be linearly proportional to the deflection between two layers, i.e.,

$$q_k = \sum_{j=1}^{N} c_{kj}(w_k - w_j) = w_k\sum_{j=1}^{N} c_{kj} - \sum_{j=1}^{N} c_{kj}w_j, \tag{57}$$

where N is the total number of layers of the multi-walled carbon nanotube and c_{kj} is the van der Waals interaction coefficient.

The van der Waals interaction coefficients can be obtained through the Lennard-Jones pair potential (Jones, 1924). Here, van der Waals interaction coefficients obtained through the Lennard-Jones pair potential by He et al. (2005) are used.

Obviously, Equation (56b) is uncoupled from the other two equations in Equation (56) such that the torsional waves in the shell are not coupled with the longitudinal and radial waves.

6.2 Longitudinal wave dispersion in multi-walled carbon nanotubes

In this section, the wave propagations of multi-walled carbon nanotubes are investigated via the second-order strain gradient shell theory.

Consider the motions governed by the coupled dynamic equations in u and w, let

$$u_k = \hat{u}_k e^{i\tilde{k}(x-ct)},\ w_k = \hat{w}_k e^{i\tilde{k}(x-ct)},\quad (k = 1,2\cdots N) \tag{58}$$

where $i \equiv \sqrt{-1}$, $\hat{u}_k$ is the amplitude of longitudinal vibration, and $\hat{w}_k$ is the amplitude of radial vibration. Substituting Equation (58) into Equations (56a) and (56c) yields

$$\left[\frac{\tilde{k}^2c^2}{c_p^2} - \tilde{k}^2 + r^2\tilde{k}^4\right]\hat{u}_k + \left[i(\tilde{k} - r^2\tilde{k}^3)\frac{\upsilon}{R}\right]\hat{w}_k = 0, \tag{59a}$$

$$\left[-\mathrm{i}(\tilde{k}-r^2\tilde{k}^3)\frac{\upsilon}{R}\right]\hat{u}_k+\left[\frac{\tilde{k}^2c^2}{c_p^2}-\frac{1}{R^2}(1-r^2\tilde{k}^2)\right]\hat{w}_k+\frac{1-v^2}{Eh}\left(\hat{w}_k\sum_{j=1}^{n}c_{kj}-\sum_{j=1}^{n}c_{kj}\hat{w}_j\right)=0\,. \tag{59b}$$

The dispersion relation can then be obtained by solving the eigenvalue equation,

$$\left[\frac{\tilde{k}^2}{c_p^2}c^2\mathbf{I}_{2N\times 2N}+\mathbf{H}_{2N\times 2N}\right]\begin{bmatrix}\hat{u}_1\\ \hat{w}_1\\ \hat{u}_2\\ \hat{w}_2\\ \vdots\\ \hat{u}_N\\ \hat{w}_N\end{bmatrix}=0\,, \tag{60}$$

where $c_p\equiv\sqrt{E/((1-\upsilon^2)\rho)}$, and $\mathbf{I}_{2N\times 2N}$ is an identity matrix and the elements in the matrix $\mathbf{H}_{2N\times 2N}$ are

$$\mathbf{H}(2k,2j)=-\frac{(1-v^2)c_{kj}}{Eh}\quad(k\neq j)\,, \tag{61a}$$

$$\mathbf{H}(2k-1,2k-1)=-\tilde{k}^2+r^2\tilde{k}^4\,, \tag{61b}$$

$$\mathbf{H}(2k-1,2k)=\mathrm{i}(\tilde{k}-r^2\tilde{k}^3)\frac{\upsilon}{R_k}\,, \tag{61c}$$

$$\mathbf{H}(2k,2k-1)=-\mathrm{i}(\tilde{k}-r^2\tilde{k}^3)\frac{\upsilon}{R_k}\,, \tag{61d}$$

$$\mathbf{H}(2k,2k)=-\frac{1}{R_k^2}(1-r^2\tilde{k}^2)+\frac{1-v^2}{Eh}\sum_{j=1}^{n}c_{kj}\,. \tag{61e}$$

The parameters of Equation (60) are as follows: $Eh=347\,\mathrm{Pa\bullet m}$, $\rho h=761\,\mathrm{kg\bullet nm/m^3}$, $r=0.0355\mathrm{nm}$, $\upsilon=0.2$.

To see the effect of the strain gradient in multi-walled carbon nanotubes clearly; two double-walled carbon nanotubes are using as examples. Equation (60) becomes

$$\begin{bmatrix}\frac{\tilde{k}^2c^2}{c_p^2}-\tilde{k}^2+r^2\tilde{k}^4 & \mathrm{i}(\tilde{k}-r^2\tilde{k}^3)\frac{\upsilon}{R_1} & 0 & 0\\ -\mathrm{i}(\tilde{k}-r^2\tilde{k}^3)\frac{\upsilon}{R_1} & \frac{\tilde{k}^2c^2}{c_p^2}-\frac{1}{R_1^2}(1-r^2\tilde{k}^2)+\frac{1-v^2}{Eh}c_{12} & 0 & -\frac{(1-v^2)c_{12}}{Eh}\\ 0 & 0 & \frac{\tilde{k}^2c^2}{c_p^2}-\tilde{k}^2+r^2\tilde{k}^4 & \mathrm{i}(\tilde{k}-r^2\tilde{k}^3)\frac{\upsilon}{R_1}\\ 0 & \frac{(1-v^2)c_{12}}{Eh} & -\mathrm{i}(\tilde{k}-r^2\tilde{k}^3)\frac{\upsilon}{R_1} & \frac{\tilde{k}^2c^2}{c_p^2}-\frac{1}{R_1^2}(1-r^2\tilde{k}^2)-\frac{1-v^2}{Eh}c_{12}\end{bmatrix}\begin{bmatrix}\hat{u}_1\\ \hat{w}_1\\ \hat{u}_2\\ \hat{w}_2\end{bmatrix}=0 \tag{62}$$

Figures 10 compare the strain gradient shell model and the classical shell model in terms of the longitudinal wave dispersion of two double-walled carbon nanotubes (with diameters of 0.68nm and 1.36nm, 6.8nm and 7.48nm, respectively). The difference between the dispersion relation given by the strain gradient shell model and the classical shell model becomes more and more obvious with increasing wave number. This is similar to the results obtained from single-walled carbon nanotubes (Wang & Hu, 2005).

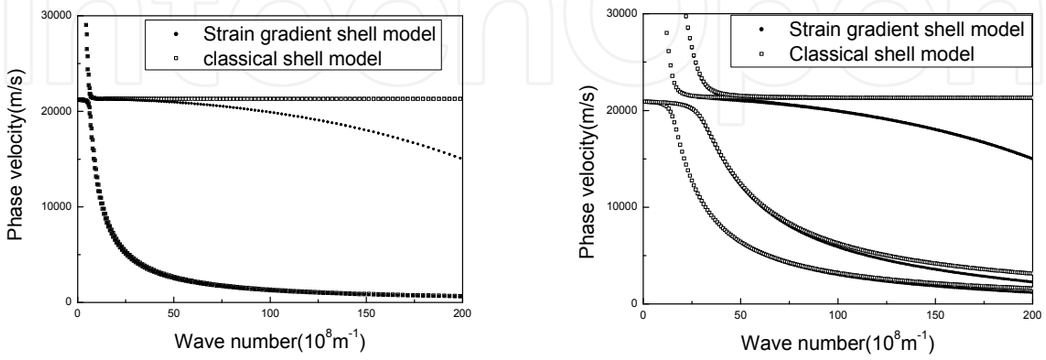

(a) A double-walled carbon nanotube with diameter inner 6.8nm, outer 7.48nm

(b) A double-walled carbon nanotube with diameter inner 0.68nm, outer 1.36nm

Fig. 10. Comparison of the strain gradient shell model and the classical shell model on the dispersion relation of double-walled carbon nanotubes(Wang *et al*. 2008b)

6.3 Group velocity of longitudinal wave in a multi-walled carbon nanotube

From Equation (59), with $\omega = c\tilde{k}$ considered, one arrives at

$$\left[\frac{\omega^2}{c_p^2}\mathbf{I}_{2N\times 2N} + \mathbf{H}_{2N\times 2N}\right]\begin{bmatrix}\hat{u}_1\\ \hat{w}_1\\ \hat{u}_2\\ \hat{w}_2\\ \vdots\\ \hat{u}_N\\ \hat{w}_N\end{bmatrix} = 0\,, \tag{63}$$

where $c_p \equiv \sqrt{E/((1-\upsilon^2)\rho)}$, $\mathbf{I}_{2N\times 2N}$ is an identity matrix and the entries in matrix $\mathbf{H}_{2N\times 2N}$ are

$$\mathbf{H}(2k, 2j) = -(1-\upsilon^2)c_{kj}/Eh, \qquad k \neq j\,, \tag{64a}$$

$$\mathbf{H}(2k-1, 2k-1) = -\tilde{k}^2 + r^2\tilde{k}^4\,, \tag{64b}$$

$$\mathbf{H}(2k-1, 2k) = \mathrm{i}(\tilde{k} - r^2\tilde{k}^3)\upsilon/R_k\,, \tag{64c}$$

$$\mathbf{H}(2k,2k-1) = -\mathrm{i}(\tilde{k} - r^2\tilde{k}^3)\upsilon/R_k \,, \tag{64d}$$

$$\mathbf{H}(2k,2k) = -\frac{1}{R_k^2}(1 - r^2\tilde{k}^2) + \frac{1-v^2}{Eh}\sum_{j=1}^{n} c_{kj} \,. \tag{64e}$$

From Equation (63), the dispersion relation between the group velocity and the wave number of longitudinal waves in a multi-walled carbon nanotube can be numerically determined through $c_g = \mathrm{d}\omega/\mathrm{d}\tilde{k}$.

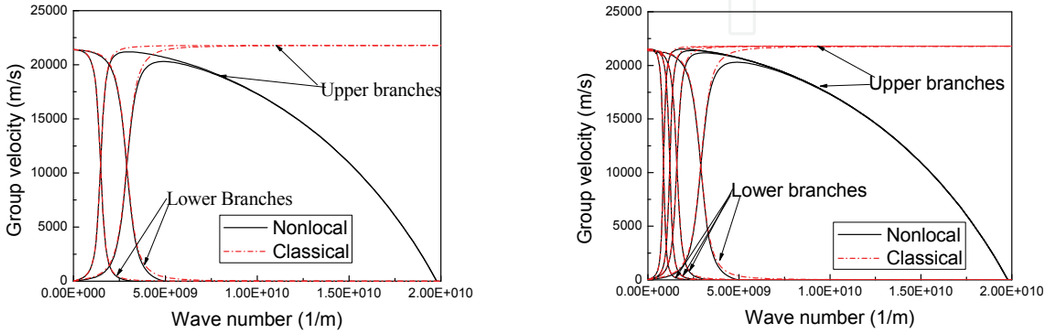

(a) A double-walled carbon nanotube with radii 0.34nm and 0.68nm

(b) A quadruple-walled carbon nanotube with radii 0.34nm, 0.68nm, 1.02nm and 1.36nm

Fig. 11. Dispersion relation between the group velocity and the wave number of longitudinal wave in multi-walled carbon nanotubes(Wang *et al*. 2008a)

Figure 11 presents the dispersion relation between the group velocity and the wave number of longitudinal waves in a double-walled carbon nanotube with the radii $R_1 = 0.34\text{nm}$ and $R_2 = 0.68\text{nm}$ respectively, and in a quadruple-walled carbon nanotube with the radii $R_1 = 0.34\text{nm}$, $R_2 = 0.68\text{nm}$, $R_3 = 1.02\text{nm}$ and $R_4 = 1.36\text{nm}$, respectively. The product of Young's modulus and the wall thickness is $Eh = 346.8\text{Pa}\cdot\text{m}$, and Poisson's ratio is $\upsilon = 0.20$ for both the double-walled carbon nanotube and the quadruple-walled carbon nanotube. In addition, one has $r = 0.0355\text{nm}$ when the axial distance between two neighboring rings of atoms reads $d = 0.123\text{nm}$. The product of mass density and the wall thickness yields $\rho h \approx 760.5\text{kg/m}^3\cdot\text{nm}$. Now, there is a slight difference between the theory of non-local elasticity and the classical theory of elasticity for the lower branches. The group velocity decreases rapidly with an increase in the wave number. When the wave number approaches to $\tilde{k}=5\times10^9\ \text{m}^{-1}$ or so, the group velocity of all these lower branches goes to zero. For the upper branches of the dispersion relation, the difference is almost invisible when the wave number is lower. However, the results of the elastic cylindrical shells remarkably deviate from those of non-local elastic cylindrical shells with an increase in the wave number. Figures 11 (a) and (b) show again the intrinsic limit of wave number yielding $\tilde{k}<2\times10^{10}\ \text{m}^{-1}$, instead of $\tilde{k}<\sqrt{12}/d\approx2.82\times10^{10}\text{m}^{-1}$.

7. Concluding remarks

This chapter presents a detailed study on the dispersion relation between the phase velocity, group velocity and the wave number for the propagation of flexural and longitudinal waves in single- and multi-walled carbon nanotubes on the basis of the elastic and the non-local elastic Timoshenko beams and cylindrical shells. The study indicates that both elastic and non-local elastic models can offer the right prediction when the wave number is lower. However, the results of the elastic model remarkably deviate from those given by the non-local elastic model with an increase of the wave number. As a result, the micro-structures play an important role in the dispersion of both longitudinal and flexural waves in single- and multi-walled carbon nanotubes.

The cut-off wave number of the dispersion relation between the group velocity and the wave number is about $2\times10^{10}\ 1/\mathrm{m}$ for both flexural and longitudinal waves in both single- and multi-walled carbon nanotubes. This fact interprets the contradiction that the direct molecular dynamics simulation can not give the dispersion relation between the phase velocity and the wave number when the wave number approaches to $2\times10^{10}\ 1/\mathrm{m}$, which is much lower than the cut-off wave number of the dispersion relation between the phase velocity and the wave number predicted by the continuum mechanics.

Propagation of waves in infinite long carbon nanotubes is discussed in this chapter. The effects of boundary on the wave propagation are not considered. It is of great interest to carry out the research on the finite length carbon nanotube, with the effects of boundary conditions taken into consideration. There is little experiment work on the wave propagation in carbon nanotube. Future experiment studies should be conducted to explore this properties and potential applications.

8. Acknowledgements

This work was supported by the National Natural Science Foundation of China under Grants 10702026.

9. References

Askes, H.; Suiker, A. S. J. & Sluys, L. J. (2002). A classification of higher-order strain-gradient models – linear analysis. *Archive of Applied Mechics,* 72, 171-188.

Brenner D. W. (1990) Empirical potential for hydrocarbons for use in simulating the chemical vapor deposition of diamond films. *Physical Review B,* 42, 9458.

Chakraborty, A. (2007). Shell element based model for wave propagation analysis in multi-wall carbon nanotubes. *International Journal of Solids and Structures,* 44, 1628-1642

Chang C. S.; Gao J. (1995). Second-gradient constitutive theory for granular material with random packing structure. *International Journal Solids and Structures,* 32(16), 2279-2293.

Cornwell C. F.; Wille L. T. (1997). Elastic properties of single-walled carbon nanotubes in compression. *Solid State Communications,* 101, 555.

Craig R. R., (1981). *Structural Dynamics* (New York: John Wiley & Sons,).

Dong, K. & Wang, X. (2006). Wave propagation in carbon nanotubes under shear deformation. *Nanotechnology,* 17, 2773-2782.

Graff, K. F. (1975). *Wave Motion in Elastic Solids*,Ohio: Ohio State University.

Girifalco L.A. & Lad, R. A. (1956). Energy of Cohesion, Compressibility, and the Potential Energy Functions of the Graphite System. *The Journal of Chemical Physics,* 25, 693

Halicioglu T. (1998). Stress Calculations for Carbon Nanotubes, *Thin solid films*, 312, 11

He X. Q.; Kitipornchai S; & Liew, K. M. (2005). Buckling analysis of multi-walled carbon nanotubes: a continuum model accounting for van der Waals interaction. *Journal of the Mechanics and Physics of Solids*, 53, 303-326.

Iijima, S. (1991). Helical microtubules of graphitic carbon. *Nature*, 354, 56-58.

Jones, J.E. (1924). The determination of molecular fields: from the variation of the viscosity of a gas with temperature. *Proceedings of the Royal Society of London A* , 106, 441.

Leach, A. R. (1996). *Molecular Modeling*, London: Addison Wesley Longman Limited

Manolis, G. D. (2000). Some basic solutions for wave propagation in a rod exhibiting non-local elasticity. *Engineering Analysis with Boundary Elements*, 24(6), 503-508.

Mindlin, R. D. (1964). Micro-structure in linear elasticity. *Archive of Rational Mechanics and Analysis,* 16(1), 51-78.

Mühlhaus, H. B. & Oka F. (1996). Dispersion and wave propagation in discrete and continuous models for granular materials. *International Journal of Solids and Structures,* 33(19), 2841-2858.

Natsuki, T.; Hayashi, T. & Endo, M. (2005). Wave propagation of carbon nanotubes embedded in an elastic medium. *Journal of Applied Physics,* 97, 044307.

Natsuki, T.; Endo, M. & Tsuda, H. (2006). Vibration analysis of embedded carbon nanotubes using wave propagation approach. *Journal of Applied Physics,* 99, 034311.

Nowinski, J. L. (1984). On a nonlocal theory of longitudinal waves in an elastic circular bar. *Acta Mechanica,* 52(3-4), 189-200.

Poncharal, P.; Wang, Z. L.; Ugarte, D. & de Heer W. A. (1999). Electrostatic Defections and Electromechanical Resonances of Carbon Nanotubes. *Science,* 283, 1513-1516.

Popov, V. N.; Van Doren, V. E. & Balkanski, M. (2000). Elastic properties of single-walled carbon nanotubes. *Physical Review B,* 61, 3078-3084.

Qian, D.; Wagner, G. J.; Liu, W. K.; Yu, M. F. & Ruoff, R. S. (2002). Mechanics of carbon nanotubes. *Applied Mechanics Review,* 55, 495-533.

Ru, C. Q. (2000). Column buckling of multiwalled carbon nanotubes with interlayer radial displacements. *Physical Review B,* 62, 16962.

Sudak, L. J. (2003). Column buckling of multiwalled carbon nanotubes using nonlocal continuum mechanics. *Journal of Applied Phys*ics, 94, 7281-7287.

Timoshenko, S. & Gere, J. (1972). *Mechanics of Material,* New York: Van Nostrand Reinhold Company.

Treacy, M. M. J.; Ebbesen, T. W. & Gibson J. M. (1996). Exceptionally high Young's modulus observed for individual carbon nanotubes. *Nature*, 381, 678-680.

Wang, C. Y.; Ru, C. Q. & Mioduchowski, A. (2005a). Free vibration of multiwall carbon nanotubes. *Journal of Applied Phys*ics, 97, 114323.

Wang, C. M.; Zhang, Y. Y.; Ramesh, S. S. & Kitipornchai, S. (2006a). Buckling analysis of micro- and nano-rods/tubes based on nonlocal Timoshenko beam theory. *Journal of Physics D: Applied Phys*ics, 39, 3904-3909.

Wang, L. F. (2005). *On some mechanics problems in one dimensional nanostructures.* Doctoral dissertation of Nanjing University of Aeronautics and Astronautics (in Chinese).

Wang, L. F. & Hu, H. Y. (2005). Flexural wave propagation in single-walled carbon nanotubes. *Physical Review B*, 71, 195412.

Wang, L. F.; Hu, H. Y., & Guo, W. L. (2006b). Validation of the non-local elastic shell model for studying longitudinal waves in single-walled carbon nanotubes. *Nanotechnology,* 17, 1408-1415.

Wang L. F.; Guo W. L.; Hu H. Y. (2008a). Group velocity of wave propagation in carbon nanotubes, *Proceedings of the Royal Society A*, 464: 1423-1438

Wang, L. F.; Liew, K. M.; He, X. Q.; Hu, Y. G.; Wang, Q.; Guo, W. L. & Hu, H. Y., (2008b), Using Model of Strain Gradient Membrane Shell to Characterize Longitudinal Wave Dispersion in Multi-Walled Carbon Nanotubes. *Journal of Computational and Theoretical Nanoscience*, 5: 1980–1988

Wang, Q. (2005b). Wave propagation in carbon nanotubes via nonlocal continuum mechanics. *Journal of Applied Physics,* 98, 124301.

Wong, E. W.; Sheehan, P.E. & Lieber, C.M. (1997). Nanobeam Mechanics: Elasticity, Strength, and Toughness of Nanorods and Nanotubes. *Science,* 277, 1971-1975.

Xie, G. Q.; Han, X. & Long, S. Y. (2006). Effect of small size on dispersion characteristics of wave in carbon nanotubes. *International Journal of Solids and Structures,* 44, 1242-1255.

Yakobson, B. I.; Brabec C. J. & Bernholc J. (1996). Nanomechanics of Carbon Tubes: Instabilities beyond Linear Response. *Physical Review Letters*, 76, 2511-2514.

Yoon, J.; Ru, C. Q. & Mioduchowski, A. (2002). Non-coaxial resonance of an isolated multiwall carbon nanotube. *Physical Review B*. 66, 233402.

Yoon, J.; Ru, C. Q. & Mioduchowski, A. (2003a). Vibration of embedded multi-wall carbon nanotubes. *Composites Science and Technology,* 63, 1533-1542.

Yoon, J.; Ru, C. Q. & Mioduchowski, A. (2003b). Sound wave propagation in multi-wall carbon nanotubes. *Journal of Applied Physics,* 93, 4801-4806.

Zhang P.; Huang Y.; Geubelle P. H.; Klein P. A. &Hwang K. C., (2002). The elastic modulus of single-walled carbon nanotubes: a continuum analysis incorporating interatomic potentials. *International Journal of Solids and Structures*, 39, 3893.

Zhang, Y. Q.; Liu, G. R. & Wang, J. S. (2004). Small-scale effects on buckling of multiwalled carbon nanotubes under axial compression. *Physical Review B*, 70, 205430.

Zhang, Y. Q.; Liu, G. R. & Xie X. Y. (2005). Free transverse vibrations of double-walled carbon nanotubes using a theory of nonlocal elasticity. *Physical Review B*, 71, 195404.

Wave Propagation in Materials for Modern Applications

Edited by Andrey Petrin

ISBN 978-953-7619-65-7
Hard cover, 526 pages
Publisher InTech
Published online 01, January, 2010
Published in print edition January, 2010

In the recent decades, there has been a growing interest in micro- and nanotechnology. The advances in nanotechnology give rise to new applications and new types of materials with unique electromagnetic and mechanical properties. This book is devoted to the modern methods in electrodynamics and acoustics, which have been developed to describe wave propagation in these modern materials and nanodevices. The book consists of original works of leading scientists in the field of wave propagation who produced new theoretical and experimental methods in the research field and obtained new and important results. The first part of the book consists of chapters with general mathematical methods and approaches to the problem of wave propagation. A special attention is attracted to the advanced numerical methods fruitfully applied in the field of wave propagation. The second part of the book is devoted to the problems of wave propagation in newly developed metamaterials, micro- and nanostructures and porous media. In this part the interested reader will find important and fundamental results on electromagnetic wave propagation in media with negative refraction index and electromagnetic imaging in devices based on the materials. The third part of the book is devoted to the problems of wave propagation in elastic and piezoelectric media. In the fourth part, the works on the problems of wave propagation in plasma are collected. The fifth, sixth and seventh parts are devoted to the problems of wave propagation in media with chemical reactions, in nonlinear and disperse media, respectively. And finally, in the eighth part of the book some experimental methods in wave propagations are considered. It is necessary to emphasize that this book is not a textbook. It is important that the results combined in it are taken “from the desks of researchers“. Therefore, I am sure that in this book the interested and actively working readers (scientists, engineers and students) will find many interesting results and new ideas.

Slavka Krautzeka 83/A
51000 Rijeka, Croatia
Phone: +385 (51) 770 447
Fax: +385 (51) 686 166
www.intechopen.com

No.65, Yan An Road (West), Shanghai, 200040, China
中国上海市延安西路65号上海国际贵都大饭店办公楼405单元
Phone: +86-21-62489820
Fax: +86-21-62489821

IntechOpen

IntechOpen